

Realizing \mathcal{PT} -symmetric non-Hermiticity with ultracold atoms and Hermitian multiwell potentials

Manuel Kreibich, Jörg Main, Holger Cartarius, and Günter Wunner
Institut für Theoretische Physik 1, Universität Stuttgart, 70550 Stuttgart, Germany
 (Received 1 August 2014; published 30 September 2014)

We discuss the possibility of realizing a *non-Hermitian*, i.e., an *open* two-well system of ultracold atoms by enclosing it within additional time-dependent wells that serve as particle reservoirs. With the appropriate design of the additional wells, \mathcal{PT} -symmetric currents can be induced to and from the inner wells, which support stable solutions. We show that interaction in the mean-field limit does not destroy this property. As a first method we use a simplified variational ansatz leading to a discrete nonlinear Schrödinger equation. A more accurate and more general variational ansatz is then used to confirm the results.

DOI: [10.1103/PhysRevA.90.033630](https://doi.org/10.1103/PhysRevA.90.033630)

PACS number(s): 03.75.Hh, 03.65.Ge, 11.30.Er

I. INTRODUCTION

Since the first realization of \mathcal{PT} -symmetric gain and loss in optical waveguides [1] much effort has been made to realize analogous systems in various fields of physics, e.g., lasers [2], electronics [3], and microwave cavities [4], and to make use of new effects arising from nonlinearity, viz., the Kerr nonlinearity in optical waveguides [5]. \mathcal{PT} symmetry originates from quantum mechanics and stands for a combined action of parity and time reversal. Despite the non-Hermiticity of \mathcal{PT} -symmetric Hamiltonians, in a certain range of parameters entirely real eigenvalue spectra exist [6]. Due to a formal analogy between quantum mechanics and electromagnetism, the formulation of \mathcal{PT} symmetry has spread to those systems, leading to the above-mentioned realizations. However, experimental verification in a genuine quantum system has not been achieved so far.

In a \mathcal{PT} -symmetric system there is a balanced gain and loss of probability density (or electromagnetic field in analog systems). According to a proposal in [7] such a quantum-mechanical system could be realized with a Bose-Einstein condensate (BEC) in a double-well potential where particles are injected into one well and removed from the other. Indeed, it could be shown that the system is ideally suited for a first experimental observation of \mathcal{PT} symmetry in a quantum system [8]. There is progress in coupling two BECs and at the same time ejecting particles [9], but an actual realization of \mathcal{PT} symmetry using a BEC is still missing.

On the other hand much theoretical work has been done on \mathcal{PT} -symmetric BECs, including the proof of existence of stable states of interacting systems [10], a microscopic treatment based on the Bose-Hubbard model [11], and a thorough investigation of the dynamics of stable and unstable regimes [12]. In contrast to injecting and removing particles from a double-well potential, one could think of a double well included in a tilted optical lattice, with an incoming and outgoing transport of particles, a so-called Wannier-Stark system [13,14]. These incoming and outgoing particle currents could in principle serve as the necessary currents for realizing a \mathcal{PT} -symmetric system.

In a recent Rapid Communication [15] we followed the simplest approach to this idea, namely, coupling two additional wells to the double-well potential (see Fig. 1), and using the arising currents as a theoretical realization of \mathcal{PT} symmetry in a quantum-mechanical system. We showed that for a

specific time-dependent choice of the well depths and coupling strengths of the additional wells, the inner wells behave exactly as the wells of a \mathcal{PT} -symmetric two-well system, thus serving as a possible experimental realization.

It is the purpose of this paper to investigate our approach more deeply, especially for the case of interacting atoms, and to formulate a more accurate method to confirm the results. In Sec. II we derive the few-mode model or discrete nonlinear Schrödinger equation (DNLSE) from the Gross-Pitaevskii equation (GPE) using a simple variational ansatz, where each well is populated by a single time-independent Gaussian function. The results are applied in Sec. III to show that a Hermitian four-mode model can be chosen such that the middle wells behave exactly as the wells of the \mathcal{PT} -symmetric two-mode model. This is exemplified for some parameters. In Sec. IV we use an extended variational ansatz for the realization of \mathcal{PT} symmetry. Still one Gaussian function per well is used, but each Gaussian function is fully dynamical in its parameters, thus giving a more accurate description of the system. The method is compared with the simple Gaussian ansatz. In Sec. V we conclude our work.

II. FROM THE GROSS-PITAEVSKII EQUATION TO A FEW-MODE MODEL

In this section we apply the steps that lead from the GPE, which describes the dynamics of a BEC at absolute zero temperature, to a DNLSE or few-mode model. First we present our ansatz and calculate the necessary integrals. To derive the equations of motion (EOMs) in a Schrödinger form we use the method of symmetric orthogonalization. In Sec. III the results are used and applied to different scenarios.

A. Simplified variational ansatz

We start with the well-known GPE

$$i\hbar\partial_t\psi(\mathbf{r},t) = \left[-\frac{\hbar^2}{2m}\Delta + V(\mathbf{r}) + g|\psi(\mathbf{r},t)|^2 \right] \psi(\mathbf{r},t). \quad (1)$$

The interaction strength is given by $g = 4\pi\hbar^2 Na/m$ with the s -wave scattering length a and particle number N . For the external multiwell potential $V(\mathbf{r})$ we use a Gaussian profile

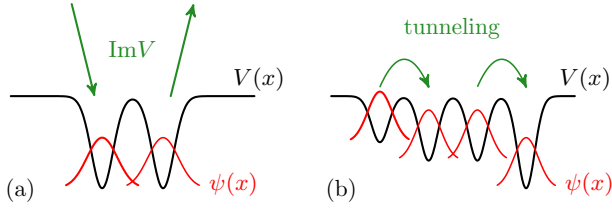


FIG. 1. (Color online) (a) Two-mode model with an imaginary potential V , where—in this case—particles are removed from the left well and injected into the right. (b) Such a system could be realized by coupling two additional wells to the system, where the tunneling currents to and from the outer wells are used as an implementation of the imaginary potential. The outer wells act as (limited) particle reservoirs and have to be chosen as time dependent.

for each well,

$$V(\mathbf{r}) = \sum_{k=1}^{N_w} V^k \exp \left[-\frac{2x^2}{w_x^2} - \frac{2y^2}{w_y^2} - \frac{2(z - s_z^k)^2}{w_z^2} \right], \quad (2)$$

with a total number of N_w wells. Each well k has the potential depth $V^k < 0$ and is displaced along the z -direction by s_z^k . Such a potential could, e. g., be created experimentally by the method presented in [16].

There is various work on how to transform the GPE (1) into a DNLS [17, 18] by integrating out the spatial degrees of freedom. In general, an ansatz of the form

$$\psi(\mathbf{r}, t) = \sum_k d^k(t) g^k(\mathbf{r}) \quad (3)$$

is used, where $d^k(t)$ is the (complex) amplitude and $g^k(\mathbf{r})$ the localized wave function in well k . Usually, a set of Wannier functions is applied [19]. In this work (Sec. III), we use a single Gaussian function for each well. With this ansatz we can derive analytical formulas for the matrix elements of the DNLS or few-mode model, and thus open an easy way to actually compute the localized wave functions by a simple energy minimization process. In Sec. IV we extend the variational ansatz to obtain more accurate results.

The simplified variational ansatz is given by the superposition of N_G Gaussian functions, one for each well, $N_w = N_G$, with

$$g^k(\mathbf{r}) = e^{-A_x^k x^2 - A_y^k y^2 - A_z^k (z - q_z^k)^2}. \quad (4)$$

The parameters $A_x^k, A_y^k, A_z^k \in \mathbb{R}$ describe the width of each Gaussian function in each direction, and $q_z^k \in \mathbb{R}$ the displacement along the z direction. We treat these parameters in this section as time independent. The time dependence of the wave function comes from the amplitude $d^k(t)$ in Eq. (3).

We insert ansatz (3) into the GPE $i\hbar\partial_t\psi = \hat{H}\psi$, multiply from the left with $(g^l)^*$, and integrate over \mathbb{R}^3 . Then, we are left with

$$i\hbar\mathbf{K}\dot{\mathbf{d}} = \mathbf{H}\mathbf{d}. \quad (5)$$

Here, the amplitudes d^k are written as a vector $\mathbf{d} = (d^1, \dots, d^{N_G})^T \in \mathbb{C}^{N_G}$. The matrix \mathbf{K} describes the overlap, and \mathbf{H} the Hamiltonian matrix elements. They are

given by the integrals (see Sec. II B for their explicit calculation)

$$K_{lk} = \langle g^l | g^k \rangle, \quad (6a)$$

$$H_{lk} = \langle g^l | \hat{H} | g^k \rangle. \quad (6b)$$

Our aim is to derive EOMs for the amplitudes in a Schrödinger form, ie., $i\hbar\dot{\mathbf{d}}_{\text{eff}} = \mathbf{H}_{\text{eff}}\mathbf{d}_{\text{eff}}$, with possibly modified amplitudes and matrix elements. Equation (5) would be of that form if \mathbf{K} were proportional to the identity matrix. Since the Gaussian functions g^k are nonorthogonal this is not the case. For that reason, we perform a symmetric orthogonalization in Sec. II C.

B. Evaluation of the integrals

The integrals occurring in Eqs. (6) are solely based on the Gaussian integral

$$\begin{aligned} \int_{-\infty}^{\infty} dx x^n e^{-Ax^2 + px} &= \frac{\partial^n}{\partial p^n} \int_{-\infty}^{\infty} dx e^{-Ax^2 + px} \\ &= \frac{\partial^n}{\partial p^n} \sqrt{\frac{\pi}{A}} e^{p^2/4A}, \quad \text{Re } A > 0. \end{aligned} \quad (7)$$

For convenience we define the abbreviations

$$A_\alpha^{kl} = A_\alpha^k + (A_\alpha^l)^*, \quad \alpha = x, y, z, \quad (8a)$$

$$\kappa_\alpha^{kl} = A_\alpha^k (A_\alpha^l)^* / A_\alpha^{kl}, \quad (8b)$$

$$\beta_\alpha^{kl} = \sqrt{\frac{A_\alpha^{kl} w_\alpha^2}{A_\alpha^{kl} w_\alpha^2 + 2}}, \quad (8c)$$

$$c^{kl} = e^{-\kappa_z^{kl} (q_z^k - q_z^l)^2}. \quad (8d)$$

The integrals of \mathbf{K} can now easily be calculated with Eq. (7) for the case $n = 0$; the result is

$$K_{lk} = \sqrt{\frac{\pi}{A_x^{kl}}} \sqrt{\frac{\pi}{A_y^{kl}}} \sqrt{\frac{\pi}{A_z^{kl}}} c^{kl}. \quad (9)$$

For the calculation of the Hamiltonian matrix \mathbf{H} , we separate it into a kinetic term \mathbf{T} , an external potential term \mathbf{V} , and an interaction term \mathbf{W} .

For the kinetic term we need integrals of the form shown in Eq. (7) with $n = 2$ and we obtain

$$T_{lk} = K_{lk} [\kappa_x^{kl} + \kappa_y^{kl} + \kappa_z^{kl} - 2(\kappa_z^{kl})^2 (q_z^k - q_z^l)^2]. \quad (10)$$

To calculate the integrals necessary for the external potential, the parameters A and p in Eq. (7) are shifted by the parameters of the external potential. The result is

$$\begin{aligned} V_{lk} &= K_{lk} \beta_x^{kl} \beta_y^{kl} \beta_z^{kl} \sum_m V^m \\ &\times \exp \left\{ -\frac{2[A_z^k (s_z^m - q_z^k) + (A_z^l)^* (s_z^m - q_z^l)]^2}{A_z^{kl} (A_z^{kl} w_z^2 + 2)} \right\}. \end{aligned} \quad (11)$$

Since the operator of the interaction potential \mathbf{W} is nonlinear, its matrix elements depend on the amplitudes d^k . With the

standard Gaussian integral we obtain

$$W_{lk} = \sum_{i,j} \tilde{W}_{lkji} (d^j)^* d^i, \quad (12)$$

where we defined the four-rank tensor

$$\begin{aligned} \tilde{W}_{lkji} = & \frac{4\pi\hbar^2 Na}{m} \sqrt{\frac{\pi}{A_x^{ijkl}}} \sqrt{\frac{\pi}{A_y^{ijkl}}} \sqrt{\frac{\pi}{A_z^{ijkl}}} \\ & \times \exp \left[-\frac{A_z^i (A_z^j)^* (q_z^i - q_z^j)^2 + A_z^i (A_z^l)^* (q_z^i - q_z^l)^2}{A_z^{ijkl}} \right] \\ & \times \exp \left[-\frac{A_z^k (A_z^j)^* (q_z^k - q_z^j)^2 + A_z^k (A_z^l)^* (q_z^k - q_z^l)^2}{A_z^{ijkl}} \right] \\ & \times \exp \left[-\frac{A_z^i A_z^k (q_z^i - q_z^k)^2 + (A_z^j)^* (A_z^l)^* (q_z^j - q_z^l)^2}{A_z^{ijkl}} \right] \end{aligned} \quad (13)$$

and the new abbreviations

$$A_\alpha^{ijkl} = A_\alpha^{ij} + A_\alpha^{kl}, \quad \alpha = x, y, z. \quad (14)$$

C. Symmetric orthogonalization

We calculated all necessary integrals for setting up the EOMs (5), which are not of the form of a Schrödinger equation (cf. Sec. II A). To achieve this, we now transform the EOMs into a Schrödinger form with the method of symmetric orthogonalization [20]: Since \mathbf{K} is Hermitian there exists a unitary transformation \mathbf{U} such that $\mathbf{D} = \mathbf{U}\mathbf{K}\mathbf{U}^\dagger$ is diagonal with real entries. Then we can construct the Hermitian matrix

$$\mathbf{X} = \mathbf{U}^\dagger \mathbf{D}^{-1/2} \mathbf{U}. \quad (15)$$

This matrix has the properties that $\mathbf{X}\mathbf{K}\mathbf{X} = \mathbb{1}$, and furthermore, if \mathbf{H} is Hermitian, so is $\mathbf{X}\mathbf{H}\mathbf{X}$. Now, we can use this matrix to transform Eq. (5) to

$$i\hbar(\mathbf{X}\mathbf{K}\mathbf{X})(\mathbf{X}^{-1}\dot{\mathbf{d}}) = (\mathbf{X}\mathbf{H}\mathbf{X})(\mathbf{X}^{-1}\mathbf{d}). \quad (16)$$

With the definitions $\mathbf{d}_{\text{eff}} = \mathbf{X}^{-1}\mathbf{d}$ and $\mathbf{H}_{\text{eff}} = \mathbf{X}\mathbf{H}\mathbf{X}$ and the above property of \mathbf{X} , we arrive at the EOM for \mathbf{d}_{eff} in Schrödinger form,

$$i\hbar\dot{\mathbf{d}}_{\text{eff}} = \mathbf{H}_{\text{eff}}\mathbf{d}_{\text{eff}} \quad (17)$$

with a Hermitian Hamiltonian matrix \mathbf{H}_{eff} (if \mathbf{H} is Hermitian). We note that the normalization condition for the wave function ψ transforms as

$$\begin{aligned} 1 & \stackrel{!}{=} \int d^3r |\psi|^2 = \mathbf{d}^\dagger \mathbf{K} \mathbf{d} = (\mathbf{X}^{-1}\mathbf{d})^\dagger (\mathbf{X}\mathbf{K}\mathbf{X})(\mathbf{X}^{-1}\mathbf{d}) \\ & = \mathbf{d}_{\text{eff}}^\dagger \mathbf{d}_{\text{eff}}. \end{aligned} \quad (18)$$

D. Application of symmetric orthogonalization and nearest-neighbor approximation

By means of symmetric orthogonalization we can transform the EOM (5) into a Schrödinger form since we know \mathbf{K} analytically. Without any further approximations the analytical expressions can become quite complicated. At this point, we introduce as usual the nearest-neighbor approximation to

obtain analytical and simple approximate expressions for \mathbf{X} and \mathbf{H}_{eff} .

The structure of the matrix elements K_{lk} [see Eq. (9)] allows for a natural approximation since the function c^{kl} drops exponentially with increasing distance apart of the wells, $|k-l|$. We say a term is of order n when $|k-l| = n$. As an approximation we consider terms only up to order $n=1$. Hence, we have $\mathbf{K} = \mathbf{K}^{(0)} + \mathbf{K}^{(1)}$ with

$$K_{lk}^{(0)} = \left(\frac{\pi}{2}\right)^{3/2} \frac{\delta_{kl}}{\sqrt{A_{x,R}^k A_{y,R}^k A_{z,R}^k}} \quad (19)$$

and

$$K_{lk}^{(1)} = \sqrt{\frac{\pi}{A_x^{kl}}} \sqrt{\frac{\pi}{A_y^{kl}}} \sqrt{\frac{\pi}{A_z^{kl}}} c^{kl} (\delta_{k,l+1} + \delta_{k+1,l}), \quad (20)$$

where $A_{\alpha,R}^k = \text{Re } A_\alpha^k$, and—for later use— $A_{\alpha,I}^k = \text{Im } A_\alpha^k$.

Using this expansion, we calculate the zeroth order of \mathbf{X} by the requirement $\mathbf{X}^{(0)}\mathbf{K}^{(0)}\mathbf{X}^{(0)} = \mathbb{1}$. We obtain

$$X_{lk}^{(0)} = \left(\frac{2}{\pi}\right)^{3/4} \sqrt[4]{A_{x,R}^k A_{y,R}^k A_{z,R}^k} \delta_{kl}. \quad (21)$$

To calculate the first order we start with

$$(\mathbf{X}^{(0)} + \mathbf{X}^{(1)})(\mathbf{K}^{(0)} + \mathbf{K}^{(1)})(\mathbf{X}^{(0)} + \mathbf{X}^{(1)}) = \mathbb{1}, \quad (22)$$

ignore second-order terms, insert the known quantities, and solve for $\mathbf{X}^{(1)}$, which yields

$$\begin{aligned} X_{lk}^{(1)} = & -\left(\frac{8}{\pi}\right)^{3/4} \frac{c^{kl}}{\sqrt{A_x^{kl}} \sqrt{A_y^{kl}} \sqrt{A_z^{kl}}} (\delta_{k,l+1} + \delta_{k+1,l}) \\ & \times \frac{\sqrt{A_{x,R}^k A_{y,R}^k A_{z,R}^k A_{x,R}^l A_{y,R}^l A_{z,R}^l}}{\sqrt[4]{A_{x,R}^k A_{y,R}^k A_{z,R}^k + \sqrt[4]{A_{x,R}^l A_{y,R}^l A_{z,R}^l}}}. \end{aligned} \quad (23)$$

Now we are able to calculate analytical approximations for the transformed Hamiltonian \mathbf{H}_{eff} . We observe that for the linear parts, i.e., the kinetic and external potential parts, the matrix elements of \mathbf{H} are proportional to \mathbf{K} , so we can write $H_{lk}^{\text{lin}} = K_{lk} h_{lk}^{\text{lin}}$ [cf. Eqs. (10) and (11)]. Thus, the orders of \mathbf{H}^{lin} are given by the orders of \mathbf{K} . Therefore, for the zeroth-order transformed Hamiltonian we obtain

$$H_{\text{eff},lk}^{\text{lin},(0)} = \sum_{m,n} X_{lm}^{(0)} K_{mn}^{(0)} X_{nk}^{(0)} h_{mn}^{\text{lin}} = h_{kk}^{\text{lin}} \delta_{kl}. \quad (24)$$

The zeroth order contributes to the linear diagonal elements of $\mathbf{H}_{\text{eff}}^{\text{lin}}$, so they can be identified with the on-site energy $E_k = h_{kk}^{\text{lin}}$. With Eqs. (10) and (11) we can write

$$\begin{aligned} E_k = & \frac{\hbar^2}{2m} (A_{x,R}^k + A_{y,R}^k + A_{z,R}^k) + V^k \beta_x^{kk} \beta_y^{kk} \beta_z^{kk} \\ & \times \exp[-2(\beta_z^{kk})^2 (s_z^k - q_z^k)^2 / w_z^2], \end{aligned} \quad (25)$$

where we considered only the term with $m=k$ in the sum in Eq. (11) to be consistent with the zeroth order.

The first-order terms of $\mathbf{H}_{\text{eff}}^{\text{lin}}$ are given by the first-order terms of the expression

$$(\mathbf{X}^{(0)} + \mathbf{X}^{(1)})(\mathbf{H}^{\text{lin},(0)} + \mathbf{H}^{\text{lin},(1)})(\mathbf{X}^{(0)} + \mathbf{X}^{(1)}), \quad (26)$$

which gives, after inserting all known quantities,

$$\begin{aligned}
 H_{\text{eff},lk}^{\text{lin},(1)} &= -2\sqrt{2} \frac{\sqrt{A_{x,R}^k A_{y,R}^k A_{z,R}^k A_{x,R}^l A_{y,R}^l A_{z,R}^l}}{\sqrt[4]{A_{x,R}^k A_{y,R}^k A_{z,R}^k} + \sqrt[4]{A_{x,R}^l A_{y,R}^l A_{z,R}^l}} \\
 &\times \left(\frac{E_k - h_{lk}}{\sqrt[4]{A_{x,R}^k A_{y,R}^k A_{z,R}^k}} + \frac{E_l - h_{lk}}{\sqrt[4]{A_{x,R}^l A_{y,R}^l A_{z,R}^l}} \right) \\
 &\times \frac{c^{kl}}{\sqrt{A_x^{kl}} \sqrt{A_y^{kl}} \sqrt{A_z^{kl}}} (\delta_{k,l+1} + \delta_{k+1,l}). \quad (27)
 \end{aligned}$$

These elements can be identified as the tunneling elements of the few-mode model, i.e., $J_{lk} = -H_{\text{eff},lk}^{\text{lin},(1)}$, since they are the super- and subdiagonal entries. The quantity h_{lk}^{lin} is given by Eqs. (10) and (11), where in v_{lk} we consider only nearest-neighbor contributions,

$$\begin{aligned}
 v_{lk} &= \beta_x^{kl} \beta_y^{kl} \beta_z^{kl} \\
 &\times \left(V^k \exp \left\{ - \frac{2[A_z^k (s_z^k - q_z^k) + (A_z^l)^* (s_z^k - q_z^l)]^2}{A_z^{kl} (A_z^{kl} w_z^2 + 2)} \right\} \right. \\
 &\left. + V^l \exp \left\{ - \frac{2[A_z^k (s_z^l - q_z^k) + (A_z^l)^* (s_z^l - q_z^l)]^2}{A_z^{kl} (A_z^{kl} w_z^2 + 2)} \right\} \right). \quad (28)
 \end{aligned}$$

So far we have calculated the matrix elements of the linear transformed Hamiltonian $\mathbf{H}_{\text{eff}}^{\text{lin}}$. We now turn our attention to the interaction part. Since the operator \mathbf{W} is nonlinear and depends on the amplitudes d^k , they must be transformed, too. For the transformed operator, we obtain

$$\begin{aligned}
 W_{\text{eff},lk} &= \sum_{i,j,m,n,p,q} X_{lm} \tilde{W}_{mnji} X_{nk} (X_{jp} d_{\text{eff}}^p)^* (X_{iq} d_{\text{eff}}^q) \\
 &= \sum_{p,q} \sum_{i,j,m,n} \underbrace{X_{lm} X_{pj} \tilde{W}_{mnji} X_{nk} X_{iq}}_{\equiv \tilde{W}_{\text{eff},lkpq}} (d_{\text{eff}}^p)^* d_{\text{eff}}^q. \quad (29)
 \end{aligned}$$

For the interaction term, we consider only on-site elements, i.e., elements with $i = j = k = l$ in \tilde{W}_{lkji} , since mainly these terms contribute to the interaction part. For the transformed four-rank tensor, we then obtain

$$\tilde{W}_{\text{eff},kkkk} = \frac{4\hbar^2 Na}{\sqrt{\pi m}} \sqrt{A_{x,R}^k A_{y,R}^k A_{z,R}^k}. \quad (30)$$

These elements are the nonlinear coupling constants $c_k = \tilde{W}_{\text{eff},kkkk}$. The whole action of the transformed Hamiltonian then reads

$$W_{\text{eff},lk} = c_k |d^k|^2 \delta_{kl}. \quad (31)$$

We have all necessary matrix elements in nearest-neighbor approximation. Using this knowledge we can calculate these elements from the Gaussian variational approach, or—vice versa—determine the parameters of the realistic potential (2) by knowing the matrix elements. As an application this is done in Sec. III. The parameters A_α^k and q_α^k can be computed by minimizing the mean-field energy of the system for a given

initial condition with

$$E_{\text{MF}} = \sum_{k,l} (d^l)^* (T_{lk} + V_{lk}) d^k + \frac{1}{2} \sum_{i,j,k,l} (d^l)^* d^k W_{lkji} (d^j)^* d^i. \quad (32)$$

For this minimization, all parameters A_α^k , q_α^k , and d^k have to be varied with the norm constraint (18), which is computationally much cheaper than a grid calculation. The results of this section could also be used to calculate the parameters of the Bose-Hubbard model.

Now that we have all the matrix elements, we can begin our actual investigation of a realization of a non-Hermitian system, first by means of few-mode models. In the following we will adopt the usual notation and write for the discrete wave function ψ_k instead of d^k .

III. FEW-MODE MODELS

A. Equivalence of the two- and four-mode models

We now return to the idea mentioned in the Introduction and sketched in Fig. 1, i.e., the embedding of a non-Hermitian double well in a closed four-well structure. Before analyzing the possibility of realizing a non-Hermitian system with a Hermitian model, we discuss the basic properties of the non-Hermitian two-mode model, which is given by

$$\mathbf{H}_2 = \begin{pmatrix} E_1 + c_1 |\psi_1|^2 & -J_{12} \\ -J_{12} & E_2 + c_2 |\psi_2|^2 \end{pmatrix} \quad (33)$$

with complex on-site energies $E_k \in \mathbb{C}$, which make the Hamiltonian non-Hermitian. This system has intensively been investigated in [21]. The time derivatives of the observables, that is, particle number $n_k = \psi_k^* \psi_k$ and particle current $j_{kl} = i J_{kl} (\psi_k \psi_l^* - \psi_k^* \psi_l)$, can be easily calculated, which gives (with $\hbar = 1$)

$$\partial_t n_1 = -j_{12} + 2n_1 \text{Im } E_1, \quad (34a)$$

$$\partial_t n_2 = j_{12} + 2n_2 \text{Im } E_2, \quad (34b)$$

$$\begin{aligned}
 \partial_t j_{12} &= 2J_{12}^2 (n_1 - n_2) + (\text{Im } E_1 + \text{Im } E_2) j_{12} \\
 &\quad + J_{12} (\text{Re } E_1 - \text{Re } E_2 + c_1 n_1 - c_2 n_2) C_{12}, \quad (34c)
 \end{aligned}$$

$$\begin{aligned}
 \partial_t C_{12} &= (\text{Im } E_1 + \text{Im } E_2) C_{12} \\
 &\quad - (\text{Re } E_1 - \text{Re } E_2 + c_1 n_1 - c_2 n_2) \tilde{j}_{12}, \quad (34d)
 \end{aligned}$$

where we defined $C_{kl} = \psi_k \psi_l + \psi_k^* \psi_l^*$ and $\tilde{j}_{kl} = i(\psi_k \psi_l^* - \psi_k^* \psi_l) = j_{12}/J_{12}$. In Eqs. (34a) and (34b) we see that the imaginary parts of the on-site energies act as additional sources or sinks for the particle flow, and the quantities $j_{e1} = 2n_1 \text{Im } E_1$ and $j_{e2} = -2n_2 \text{Im } E_2$ can be identified as currents to and from the environment; thus, this Hamiltonian describes an open quantum system.

The general solutions for the nonlinear model (33) are calculated in [21]. For convenience we discuss only the results of the linear, i.e., noninteracting, case ($c_1 = c_2 = 0$). Then the eigenvalues are given by

$$E_\pm = \frac{E_1 + E_2}{2} \pm \sqrt{J_{12}^2 + \frac{(E_1 - E_2)^2}{2}}. \quad (35)$$

The requirement for \mathcal{PT} symmetry leads to the condition $E_1 = E_2^*$, which is for instance fulfilled by $E_1 = i\Gamma$ and $E_2 = -i\Gamma$, a situation with balanced gain and loss. Then the eigenvalues are $E_{\pm} = \sqrt{J_{12}^2 - \Gamma^2}$. For $\Gamma < J_{12}$ they are real, whereas for $\Gamma > J_{12}$ the \mathcal{PT} symmetry is broken and the eigenvalues are purely imaginary.

It is now our main purpose to investigate whether the behavior of the non-Hermitian two-mode model (33) can be described by a Hermitian four-mode model, which is given by

$$\mathbf{H}_4(t) = \begin{pmatrix} E_0(t) & -J_{01}(t) & 0 & 0 \\ -J_{01}(t) & E_1 & -J_{12} & 0 \\ 0 & -J_{12} & E_2 & -J_{23}(t) \\ 0 & 0 & -J_{23}(t) & E_3(t) \end{pmatrix} + \text{diag}(c_0|\psi_0|^2, c_1|\psi_1|^2, c_2|\psi_2|^2, c_3|\psi_3|^2). \quad (36)$$

Two additional wells are coupled to the system; they act as a particle reservoir for the inner wells. The on-site energies and tunneling elements of the outer wells may be time dependent. Since this model is Hermitian, the on-site energies are real, $E_k \in \mathbb{R}$.

To derive a relationship between the two- and four-mode models we calculate the time derivatives of the same observables as in the two-mode model, which yields

$$\partial_t n_1 = j_{01} - j_{12}, \quad (37a)$$

$$\partial_t n_2 = j_{12} - j_{23}, \quad (37b)$$

$$\begin{aligned} \partial_t j_{12} &= 2J_{12}^2(n_1 - n_2) - J_{12}(J_{01}C_{02} - J_{23}C_{13}) \\ &\quad + J_{12}(E_1 - E_2 + c_1n_1 - c_2n_2)C_{12}, \end{aligned} \quad (37c)$$

$$\partial_t C_{12} = J_{01}\tilde{j}_{02} - J_{23}\tilde{j}_{13} - (E_1 - E_2 + c_1n_1 - c_2n_2)\tilde{j}_{12}. \quad (37d)$$

Comparing with Eqs. (34) we find that for the two-mode model the following condition must hold:

$$\text{Im } E_1 = -\text{Im } E_2 \Rightarrow E_1 = E_2^*. \quad (38)$$

This means that only the \mathcal{PT} -symmetric two-mode model, as discussed above, may be simulated by the four-mode model. From now on we write $E_1 = i\Gamma$ and $E_2 = -i\Gamma$ with $\Gamma \in \mathbb{R}$. Furthermore, the real parts of the on-site energies E_1 and E_2 and the coupling element J_{12} have to agree between the two models. We are then left with the following conditions:

$$j_{01} = 2\Gamma n_1, \quad (39a)$$

$$j_{23} = 2\Gamma n_2, \quad (39b)$$

$$0 = J_{01}C_{02} - J_{23}C_{13}, \quad (39c)$$

$$0 = J_{01}\tilde{j}_{02} - J_{23}\tilde{j}_{13}. \quad (39d)$$

To summarize at this point, if these conditions are fulfilled at every time, the two middle wells of the Hermitian four-mode model behave exactly as the wells of the \mathcal{PT} -symmetric two-mode model. These four conditions seem to be independent, but we shall see in Appendix A that Eq. (39d) follows if Eqs. (39a)–(39c) are fulfilled.

We now have to make clear that these conditions can indeed be fulfilled by giving suitable time dependencies to the elements of the four-mode Hamiltonian. Equation (39c)

can simply be fulfilled by choosing

$$J_{01}(t) = dC_{13}(t), \quad J_{23}(t) = dC_{02}(t), \quad (40)$$

where $d \neq 0$ is a real, time-independent quantity. The tunneling elements are then time dependent. With J_{01} and J_{23} determined there are no free parameters left to fulfill Eqs. (39a) and (39b). Instead, we can set the time derivatives of these equations with the help of the remaining on-site energies E_0 and E_3 . We calculate the time derivatives of j_{01} and j_{23} using the Schrödinger equation, which yields

$$\begin{aligned} \partial_t j_{01} &= (\partial_t J_{01})\tilde{j}_{01} + 2J_{01}^2(n_0 - n_1) + J_{01}J_{12}C_{02} \\ &\quad + J_{01}(E_0 - E_1 + c_0n_0 - c_1n_1)C_{01} \stackrel{!}{=} \partial_t j_{01}^{\text{tar}}, \end{aligned} \quad (41a)$$

$$\begin{aligned} \partial_t j_{23} &= (\partial_t J_{23})\tilde{j}_{23} + 2J_{23}^2(n_2 - n_3) - J_{23}J_{12}C_{13} \\ &\quad + J_{23}(E_2 - E_3 + c_2n_2 - c_3n_3)C_{23} \stackrel{!}{=} \partial_t j_{23}^{\text{tar}}, \end{aligned} \quad (41b)$$

with the target currents determined by Eqs. (39a) and (39b). The time derivatives of the tunneling elements J_{01} and J_{23} are given by

$$\begin{aligned} \partial_t J_{01} &= d\partial_t C_{13} \\ &= d(J_{01}\tilde{j}_{03} + J_{12}\tilde{j}_{23} - J_{23}\tilde{j}_{12}) \\ &\quad + d(E_3 - E_1 + c_3n_3 - c_1n_1)\tilde{j}_{13}, \end{aligned} \quad (42a)$$

$$\begin{aligned} \partial_t J_{23} &= d\partial_t C_{02} \\ &= d(J_{01}\tilde{j}_{12} - J_{12}\tilde{j}_{01} - J_{23}\tilde{j}_{03}) \\ &\quad + d(E_2 - E_0 + c_2n_2 - c_0n_0)\tilde{j}_{02}. \end{aligned} \quad (42b)$$

Inserting these into Eqs. (41), the on-site energies E_0 and E_3 are determined by a linear set of equations,

$$\begin{pmatrix} C_{01}C_{13} & \tilde{j}_{01}\tilde{j}_{13} \\ -\tilde{j}_{02}\tilde{j}_{23} & -C_{02}C_{23} \end{pmatrix} \begin{pmatrix} E_0 \\ E_3 \end{pmatrix} = \begin{pmatrix} v_0 \\ v_3 \end{pmatrix}, \quad (43)$$

with the entries

$$\begin{aligned} v_0 &= \partial_t j_{01}^{\text{tar}}/d - J_{12}\tilde{j}_{23} - d(C_{13}\tilde{j}_{03} - C_{02}\tilde{j}_{12})\tilde{j}_{01} \\ &\quad - 2dC_{13}^2(n_0 - n_1) - J_{12}C_{02}C_{13} \\ &\quad - (c_3n_3 - c_1n_1)\tilde{j}_{01}\tilde{j}_{13} - (c_0n_0 - c_1n_1)C_{01}C_{13}, \end{aligned} \quad (44a)$$

$$\begin{aligned} v_3 &= \partial_t j_{23}^{\text{tar}}/d + J_{12}\tilde{j}_{01} - d(C_{13}\tilde{j}_{12} - C_{02}\tilde{j}_{03})\tilde{j}_{23} \\ &\quad - 2dC_{02}^2(n_2 - n_3) + J_{12}C_{02}C_{13} \\ &\quad - (c_2n_2 - c_0n_0)\tilde{j}_{02}\tilde{j}_{23} - (c_2n_2 - c_3n_3)C_{02}C_{23}, \end{aligned} \quad (44b)$$

where we set $E_1 = E_2 = 0$, since—as discussed above—the real parts of these elements have to agree between the two- and four-mode models.

We have to note that by means of the on-site energies E_0 and E_3 we do not fix the currents, but their time derivatives. For this reason the initial probabilities and currents have to be chosen such that they fulfill the conditions (39). In the following section we apply these results to obtain solutions for different starting conditions.

B. Results

Before presenting our results we give the necessary initial conditions. We insert the definition of the particle current and the solutions for the tunneling elements (40) into the two

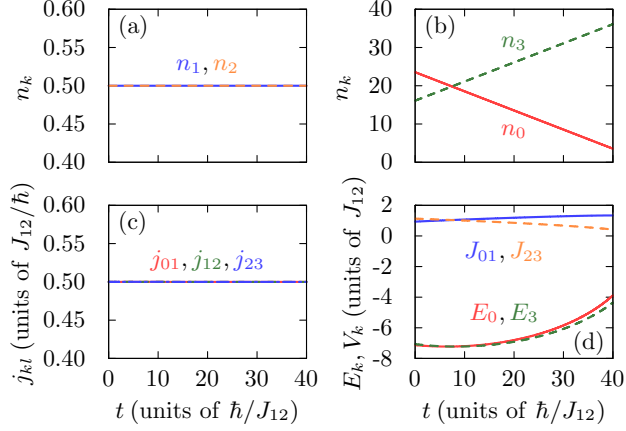


FIG. 2. (Color online) Realization of a stationary \mathcal{PT} -symmetric solution within the four-mode model. (a) Particle numbers in well 1 (solid) and well 2 (dashed) both equal to $1/2$. (b) Particle numbers in well 0 (solid) and well 3 (dashed). (c) Particle currents j_{01} (solid), j_{12} (dashed), and j_{23} (dash-dotted) in units of J_{12}/\hbar . (d) Tunneling elements J_{01} (solid), J_{23} (dashed) and on-site energies E_0 (solid), E_3 (dashed), in units of J_{12} .

equations (39a) and (39b) and express everything in terms of the wave function ψ_k . We are allowed to choose the global phase of the initial wave function, so we choose $\psi_2^I = 0$. We assume the real parts ψ_0^R and ψ_3^R to be arbitrary but fixed. We are left with (after simple rearrangement)

$$\psi_3^I = \frac{\Gamma}{2d\psi_0^R}, \quad (45a)$$

$$\psi_0^I = \frac{\psi_0^R \psi_1^I}{\psi_1^R} - \frac{\Gamma n_1}{2d\psi_1^R (\psi_1^R \psi_3^R + \psi_1^I \psi_3^I)}. \quad (45b)$$

Now, the wave function ψ_k fulfills the necessary conditions and with the time-dependencies of the matrix elements from Sec. III A we can simulate the \mathcal{PT} -symmetric two-mode model.

First we consider a stationary solution in the noninteracting case [cf. Eq. (35)] for $\Gamma/J_{12} = 0.5$. Figure 2 shows the results. As expected the particle numbers in the two middle wells are both equal and constant in time (with normalization $n_1 + n_2 = 1$), as well as the particle currents. For this reason, the number of particles decreases (left well) or increases (right well) linearly, with the slopes $\dot{n}_0 = -\Gamma/\hbar$ and $\dot{n}_3 = \Gamma/\hbar$, respectively. The matrix elements of the four-mode model vary slightly in time. Thus, we have shown that the conditions (39) can be fulfilled for a finite time.

As a second example we prepare a nonstationary solution at $t = 0$, with $\psi_1(0) = \sqrt{0.6}$ and $\psi_2(0) = \sqrt{0.4}$ (see Fig. 3). In this case the particle numbers in the two middle wells oscillate in time with a phase difference $\Delta\phi < \pi$ leading to a nonconstant total number of particles, which is a typical feature of \mathcal{PT} -symmetric systems. Since well 0 acts as a particle reservoir the number of particles decreases and gets close to zero up to the point where the linear system of equations (43) cannot be fulfilled anymore (the determinant of the coefficient matrix equals zero). This shows that the time available for a simulation of \mathcal{PT} symmetry with a reservoir is limited. The matrix elements in this case show a quasioscillatory behavior.

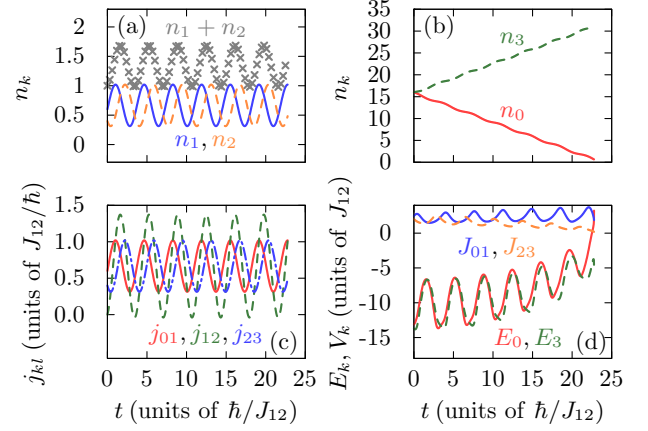


FIG. 3. (Color online) As Fig. 2, but for oscillatory dynamics. Additionally, the total number of particles $n_1 + n_2$ is plotted as crosses in (a). As the particle number in the reservoir well 0 decreases and gets close to zero, the conditions cannot be fulfilled anymore and the simulation breaks down.

Next, we consider a system with attractive interaction $c_i = -1$. In such a system it is known that the ground state changes its stability in an additional bifurcation (for a repulsive interaction, the excited state changes its stability) [12]. This phenomenon is highly correlated with the occurrence of self-trapping states. In our exemplary 2×2 system [Eq. (33)] the ground state is already unstable for the given interaction strength, so that the ground state with a small perturbation is expected to collapse. The calculation is shown in Fig. 4. The particle number n_1 increases exponentially, which marks the beginning of collapse. To support the exponential increase, the particle number in the reservoir n_0 is decreasing exponentially, so that the simulation breaks down after a quite short time interval. The matrix elements now show a rather complex time dependency.

As the last example we calculate an experimentally more realistic scenario. Up to now—as mentioned above—we had to start with appropriate wave functions in order to obtain

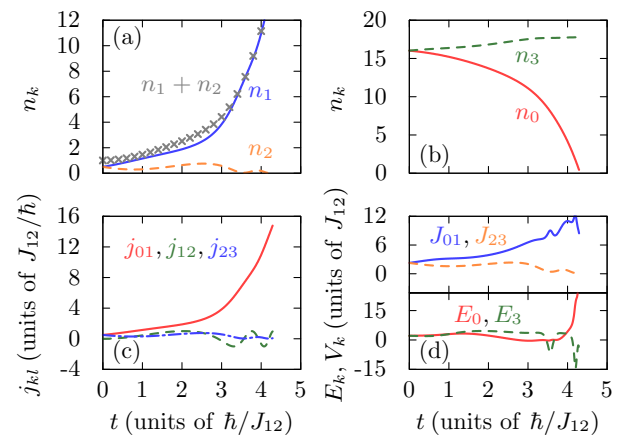


FIG. 4. (Color online) As Fig. 2, but for the interacting case ($c_i = -1$), which leads to a collapsing dynamics, indicating a change of stability. The reservoir empties in a short time domain such that the time available for \mathcal{PT} symmetry is quite short.

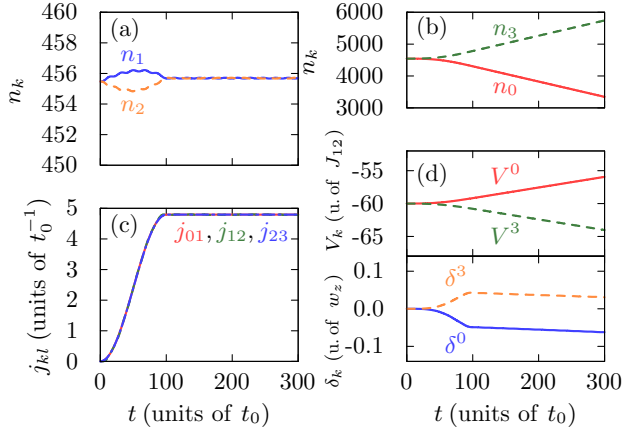


FIG. 5. (Color online) As Fig. 2, but for an adiabatic current ramp ($\Gamma_f/J_{12} = 0.5$, $t_f/t_0 = 60$) for realistic parameters of the external potential. Instead of the matrix elements, in (d) we show the parameters of the potential; δ^k marks the displacement from equidistant potential wells. There is a total number of particles of $N = 10^4$. See the text for units.

\mathcal{PT} symmetry. This is nearly impossible in an experiment. To overcome this, we use an *adiabatic* change of the \mathcal{PT} parameter from zero to its target value. We start at the ground state of the Hermitian four-mode model (with $\Gamma = 0$) and increase Γ to its target value Γ_f . If this change is slow enough, we arrive approximately at the \mathcal{PT} -symmetric ground state. The specific time dependence we use is $\Gamma(t) = \Gamma_f[1 - \cos(\pi t/t_f)]/2$ for $t \in [0, t_f]$.

In the following we simulate a condensate of $N = 10^5$ atoms of ^{87}Rb . We use units based on the potential width in the z direction, w_z , which we set as $w_z = 1 \mu\text{m}$. The basic unit of energy is $E_0 = \hbar^2/mw_z^2$, which yields $E_0/h = 116 \text{ Hz}$. The basic unit of time is $t_0 = mw_z^2/\hbar = 1.37 \text{ ms}$. The wells have widths of $w_x = w_y = 4w_z = 4 \mu\text{m}$, and are initially positioned equidistantly with a distance of $1.8w_z = 1.8 \mu\text{m}$. The potential depths are given by $V^0 = V^3 = -60E_0$ and $V^1 = V^2 = -45E_0$. We use a scattering length of $a = 2.83a_B$ with a_B being the Bohr radius.

We calculate the adiabatic ramp for $\Gamma_f/J_{12} = 0.5$ and $t_f/t_0 = 60$. The results are shown in Fig. 5. The total particle number and currents are scaled to a particle number of $N = 10^5$, the currents are given in units of $1/t_0$, and the potential depths in units of E_0 . Instead of the *positions* of the potential wells we plot the *difference* of the position from its initial value, $\delta^k = s_z^k - s_z^k(t=0)$. By means of the relations derived in Sec. II we can transform from the calculated matrix elements to the parameters of the external potential.

After a time t_f an approximate \mathcal{PT} -symmetric state is obtained. This can be seen by the constant number of particles in the middle wells, despite increasing and decreasing numbers in wells 3 and 0, respectively, which is a clear sign of \mathcal{PT} symmetry, also in a possible experiment. The potential depths of the outer wells have to be adjusted in a simple way; the positions vary within a few percent of the distance apart of the wells. This shows that the simple four-mode model can be used to describe a realistic scenario and to obtain the necessary parameters of the external potential.

We have applied our results from Sec. III A to different initial conditions and system parameters and have shown that it is indeed possible to realize a \mathcal{PT} -symmetric system with a Hermitian four-mode model. In the following section we investigate this scenario in the framework of the GPE and a variational ansatz with Gaussian functions. In particular we verify that the results agree with those from this section.

IV. VARIATIONAL ANSATZ WITH GAUSSIAN FUNCTIONS

A. Variational ansatz and equations of motion

After the simple approach in the previous section we now investigate the possible realization in the framework of the GPE with an extended variational ansatz. We use a superposition of Gaussian functions, where—in contrast to the simpler approach of Sec. II A—all variational parameters are considered as time dependent,

$$\psi = \sum_k e^{-(r-q^k)^T \mathbf{A}^k (r-q^k) + i \mathbf{p}^k (r-q^k) - \gamma^k}. \quad (46)$$

The matrices $\mathbf{A}^k = \text{diag}(A_x^k, A_y^k, A_z^k) \in \mathbb{C}^{3 \times 3}$ describe the width of each Gaussian function in each direction, the vectors $\mathbf{q}^k = (0, 0, q_z^k)^T \in \mathbb{R}^3$ and $\mathbf{p}^k = (0, 0, p_z^k)^T \in \mathbb{R}^3$ the position and momentum, respectively, and the scalar quantities $\gamma^k \in \mathbb{C}$ the amplitude and phase. This variational ansatz can describe a much richer dynamics than the ansatz (4) and thus we expect more accurate results.

The equations of motion follow from the time-dependent variational principle in the formulation of McLachlan [22], which states that the quantity

$$I = \|i\hbar\dot{\phi} - \hat{H}\psi\|^2 \quad (47)$$

must be minimized with respect to ϕ and $\phi = \dot{\psi}$ is set afterwards. Details of the necessary calculation can be found in Ref. [23], where the ansatz (46) has been used to study the collision of anisotropic solitons in a BEC. The EOMs are given by

$$i\hbar \sum_k \left\langle \frac{\partial \psi}{\partial z_l} \left| \frac{\partial \psi}{\partial z_k} \right. \right\rangle \dot{z}_k = \left\langle \frac{\partial \psi}{\partial z_l} \left| \hat{H} \right. \right\rangle \psi, \quad (48)$$

where $\mathbf{z} = (A_x^1, \dots, \gamma^{N_G})^T$ is the vector of all variational parameters. Stationary solutions are given by fixed points of (48), whereas the dynamics can be calculated by integrating Eq. (48) with a numerical integrator.

In Sec. III we started our considerations by calculating the time derivatives of the observables. In the case of the continuous GPE with a non-Hermitian potential this leads to the modified equation of continuity

$$\dot{\rho} + \text{div } \mathbf{j} = 2\rho \text{Im } V, \quad (49)$$

with $\rho = |\psi|^2$ and $\mathbf{j} = \hbar(\psi^* \nabla \psi - \psi \nabla \psi^*)/2mi$. The imaginary part of the potential acts as an additional source or sink for the probability flow. Instead of adjusting the matrix elements, we need to adjust the parameters of the external potential. Since Eq. (49) is given on the whole space \mathbb{R}^3 , one would need to change the external potential at every point in space, which is not manageable, either in theory or in an experiment.

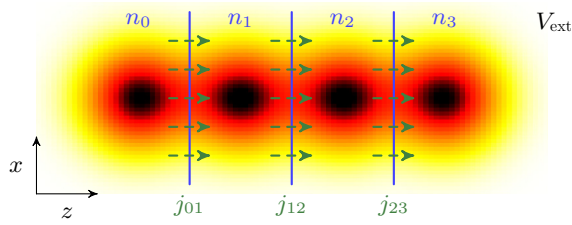


FIG. 6. (Color online) External potential V_{ext} ; the darker, the deeper the potential. The wells are separated into regions by walls at positions right in the middle between two minima. The integral over $|\psi|^2$ in a region k is the particle number n_k ; the current through a wall is denoted by $j_{k,k+1}$. See the text for exact definitions. With this separation we obtain a formulation analogous to the four-mode model (Sec. III).

To overcome this problem we use the results of Sec. III as a road map for this continuous system. For that, we separate the individual wells by walls between two minima of the potential at positions $z_k = (s_z^k + s_z^{k+1})/2$ for $k = 1, 2, 3$, $z_0 \rightarrow -\infty$, and $z_4 \rightarrow \infty$ (see Fig. 6). To obtain time derivatives of discrete observables as in the few-mode model, we integrate the continuity equation for the Hermitian four-well potential over a volume

$$V^k = \{(x, y, z)^T \mid -\infty < x, y < \infty, z_{k-1} < z < z_k\}. \quad (50)$$

This yields

$$\begin{aligned} \partial_t \iiint_{V^k} d^3r \rho &= - \iiint_{V^k} d^3r \operatorname{div} \mathbf{j} \\ &= - \iint_{\partial V^k} dA \cdot \mathbf{j}. \end{aligned} \quad (51)$$

The integral on the left-hand side can be interpreted as the number of particles in well k . On the right-hand side we used Gauss's theorem. The surface integrals are over a box, where the areas in the x - z and y - z planes go to infinity. We assume that the current \mathbf{j} also vanishes at infinity, so only the integrals over the two surfaces in the x - y plane contribute. Thus, we can write

$$\partial_t n_k = - \int_{-\infty}^{\infty} dx \int_{-\infty}^{\infty} dy [j_z(x, y, z_k) - j_z(x, y, z_{k-1})]. \quad (52)$$

The integral over the z component of \mathbf{j} evaluated at z_k represents the current from well k to well $k+1$, which we write as $j_{k,k+1}$; for z_{k-1} this represents the current from well $k-1$ to well k , $j_{k-1,k}$. We finally obtain from the continuity equation

$$\partial_t n_k = j_{k-1,k} - j_{k,k+1}, \quad (53)$$

where $j_{-1,0} = j_{3,4} = 0$.

Therefore, with Eq. (53) we have an equation analogous to that for the few-mode model (37). We can use the same method to realize a \mathcal{PT} -symmetric system. At every time step of the numerical integration of the equations of motion (48) we vary the parameters of the external potential such that the observables show the desired behavior. This is done via a nonlinear root search, in contrast to the analytical solutions of Sec. III A. In Sec. III B we showed that the positions of the outer wells barely needed to be adjusted. As a simplification we vary only

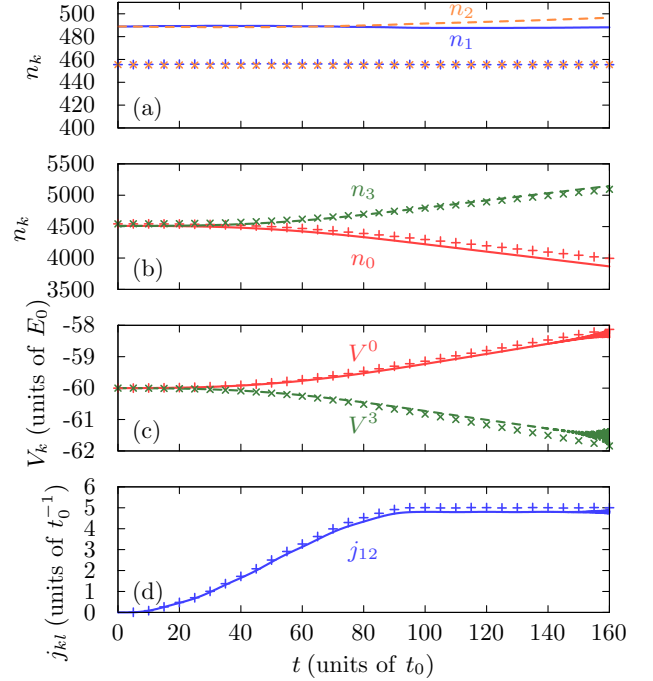


FIG. 7. (Color online) Adiabatic current ramp calculated with variational ansatz (lines) and four-mode model (crosses) for the same system. Shown are (a) particle numbers in the middle wells, (b) particle numbers in the outer wells, (c) potential depths of the outer wells in units of E_0 , and (d) particle current j_{12} . There are small deviations, but overall the four-mode model is a valid approximation compared to the variational ansatz.

the depths of the outer wells V^0 and V^3 and demand that the outer currents j_{01} and j_{23} reach the desired values. We are left with a two-dimensional root search. In the following section we determine the realization of \mathcal{PT} symmetry within the GPE and compare the results with those of the few-mode model.

B. Results and comparison with few-mode models

We use the variational ansatz to simulate the adiabatic current ramp of Sec. III B (with the same parameters) for a BEC in a four-well potential. For simplification, we do not give a specific value of the \mathcal{PT} parameter Γ but a target particle current of $j^{\text{tar}} = 5/t_0$. Figure 7 shows the results. It is not *a priori* clear whether the quantity $n_k = (d_{\text{eff}}^k)^* d_{\text{eff}}^k$ —resulting from the *transformed amplitudes* of the simplified variational approach—can be compared with the *integrated probability density* n_k of the extended variational approach. We show in Appendix B that this comparison is indeed possible and reasonable.

Overall, there is the same qualitative behavior between the two approaches. The particle number in the middle wells is slightly underestimated in the four-mode model due to its origin as an approximation. Because of the fixed positions of the outer wells for the variational approach, n_1 and n_2 are not exactly equal, but the difference is small compared to the absolute number. We can conclude that we can now also create an (approximate) \mathcal{PT} -symmetric state within the variational

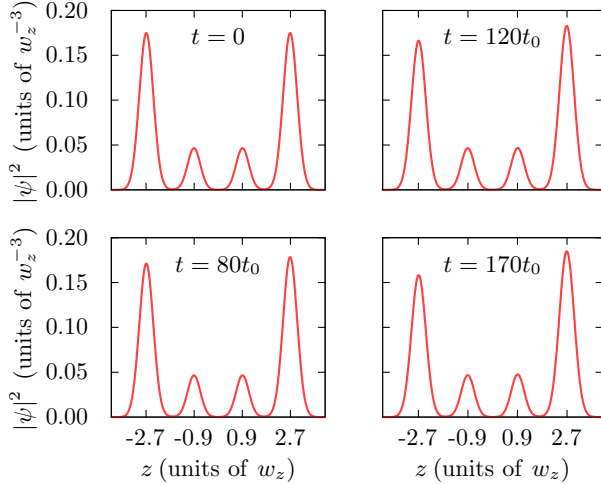


FIG. 8. (Color online) Modulus squared of the wave function $|\psi|^2$ at $x, y = 0$ for different times t . The amplitudes of the outer parts increase or decrease, whereas the amplitudes in the middle wells stay constant, a clear sign of \mathcal{PT} symmetry, as also in an experiment.

approach and verify that the results from the four-mode model are a good approximation.

The variational approach gives us access to the wave function at each time step (see Fig. 8). As indicated by the particle numbers in Fig. 7, the amplitudes in the middle wells stay almost constant, whereas the amplitudes in the outer wells increase or decrease in time. This could also be measured in an experiment and could serve as a proof of realized \mathcal{PT} symmetry.

V. CONCLUSION

By means of a simple variational ansatz—with localized time-independent Gaussian functions—and the method of symmetric orthogonalization we could transform the GPE for a multiwell potential to a simple few-mode model. The parameters of the variational ansatz are obtained by an energy minimization process in a computationally cheap way. With the results one can, on the one hand, calculate the elements of the few-mode model for a specific system, and, on the other, determine the parameters of the external potential by knowing the time-dependent matrix elements.

These results are applied to the \mathcal{PT} -symmetric two-mode model and to the Hermitian four-mode model. With this model we could show that the four-mode model can be designed in such a way that the middle wells behave exactly as the two wells of the \mathcal{PT} -symmetric two-mode model. Thus, this Hermitian (closed) system can be used as a possible realization of a quantum-mechanical \mathcal{PT} -symmetric system. With an extended Gaussian variational ansatz—with full time-dependent Gaussian functions, which can describe a much richer dynamics—we confirmed the qualitative results of the few-mode model.

In this paper we applied the idea of embedding a two-well system into a closed system for the simplest case. It is possible for future work to use a greater embedding which could result in a simpler time dependence of the additional parameters. The ideas presented in this paper could also serve as a possible

road map for an investigation of the Bose-Hubbard model and its many-particle effects.

ACKNOWLEDGMENTS

This work was supported by DFG. M.K. is grateful for support from the Landesgraduiertenförderung of the Land Baden-Württemberg.

APPENDIX A: ANALYTICAL CONSIDERATIONS

In Sec. III A we derived four conditions [Eqs. (39)] such that the Hermitian four-mode model can simulate the \mathcal{PT} -symmetric two-mode model. However, only three of them are independent, which will be shown in this appendix. For that, we need the relations

$$C_{jj}\tilde{J}_{ik} = C_{ij}\tilde{J}_{jk} + \tilde{J}_{ij}C_{jk}, \quad (\text{A1a})$$

$$C_{jj}C_{ik} = C_{ij}C_{jk} - \tilde{J}_{ij}\tilde{J}_{jk}, \quad (\text{A1b})$$

which can be proved by simply inserting the definitions of these quantities.

We start with Eqs. (39a) and (39b), insert the solutions (40), take the square, and use Eqs. (A1). We get

$$\tilde{J}_{01}^2\tilde{J}_{23}^2 + \frac{2\Gamma}{d}\tilde{J}_{12}\tilde{J}_{01}\tilde{J}_{23} - C_{12}^2\frac{n_3}{n_1}\tilde{J}_{01}^2 + \frac{4\Gamma^2}{d^2}n_1n_2 = 0, \quad (\text{A2a})$$

$$\tilde{J}_{01}^2\tilde{J}_{23}^2 + \frac{2\Gamma}{d}\tilde{J}_{12}\tilde{J}_{01}\tilde{J}_{23} - C_{12}^2\frac{n_0}{n_2}\tilde{J}_{23}^2 + \frac{4\Gamma^2}{d^2}n_1n_2 = 0. \quad (\text{A2b})$$

Taking the difference yields

$$\tilde{J}_{23}^2 = \frac{n_2n_3}{n_0n_1}\tilde{J}_{01}^2 \Leftrightarrow \tilde{J}_{23} = s_3\sqrt{\frac{n_2n_3}{n_0n_1}}\tilde{J}_{01}, \quad (\text{A3})$$

where $s_3 = \pm 1$ gives the sign of \tilde{J}_{23} compared to \tilde{J}_{01} . Inserting this result into Eq. (A2a) gives a fourth-order polynomial equation for \tilde{J}_{01} . The result is

$$\tilde{J}_{01} = s_2\sqrt{2n_0n_1[1 - \alpha + s_1\sqrt{(1 - \alpha)^2 - \beta^2}]}, \quad (\text{A4})$$

with the definitions

$$\alpha = \frac{\gamma}{2}\left(\beta + \frac{\gamma}{2}\right), \quad (\text{A5a})$$

$$\beta = s_3\frac{\Gamma}{d}\frac{1}{\sqrt{n_0n_3}}, \quad (\text{A5b})$$

$$\gamma = \frac{\tilde{J}_{12}}{\sqrt{n_1n_2}}. \quad (\text{A5c})$$

Using Eqs. (A1) we can find all other quantities \tilde{J}_{kl} and C_{kl} , especially those needed for the investigation of the fourth condition $J_{01}\tilde{J}_{02} - J_{23}\tilde{J}_{13} = dC_{13}\tilde{J}_{02} - dC_{02}\tilde{J}_{23}$,

$$C_{02} = s_2\text{sgn } d\sqrt{2n_0n_2[1 - \alpha - s_1\sqrt{(1 - \alpha)^2 - \beta^2}]}, \quad (\text{A6a})$$

$$C_{13} = s_2\text{sgn } d\sqrt{2n_1n_3[1 - \alpha - s_1\sqrt{(1 - \alpha)^2 - \beta^2}]}, \quad (\text{A6b})$$

$$\tilde{J}_{02} = s_6\sqrt{2n_0n_2[1 + \alpha + s_1\sqrt{(1 - \alpha)^2 - \beta^2}]}, \quad (\text{A6c})$$

$$\tilde{J}_{13} = s_6\sqrt{2n_1n_3[1 + \alpha + s_1\sqrt{(1 - \alpha)^2 - \beta^2}]}. \quad (\text{A6d})$$

All signs s_i are determined by the phases of the initial wave function. We can now calculate the fourth condition and find

$$J_{01}\tilde{J}_{02} - J_{23}\tilde{J}_{13} = 0. \quad (\text{A7})$$

Thus, the first three conditions of Eqs. (39) imply the validity of the fourth one. With the results of the matrix elements of Sec. III A, namely, J_{01} , J_{23} , E_0 , and E_3 , we find an exact equivalence of the two- and four-mode models also for interacting atoms. Furthermore, with the results of this appendix, we can calculate these matrix elements, once the quantities n_1 , n_2 , and \tilde{J}_{12} are known.

APPENDIX B: COMPARISON OF PROBABILITIES FOR FEW-MODE MODEL AND GAUSSIAN FUNCTIONS

As discussed in Sec. IV B it is not *a priori* clear whether we can compare the particle numbers obtained from the four-mode model and the extended variational approach. In this appendix we take a closer look at both quantities.

The transformation of the amplitudes from the four-mode model, resulting from symmetric orthogonalization, is given by the inverse of the matrix \mathbf{X} (cf. Sec. II C),

$$d_{\text{eff}}^l = \sum_k (\mathbf{X}^{-1})_{lk} d^k = \sum_k [(\mathbf{X}^{-1})_{lk}^{(0)} + (\mathbf{X}^{-1})_{lk}^{(1)}] d^k. \quad (\text{B1})$$

The individual orders of the inverse matrix can easily be calculated; we get

$$\begin{aligned} (\mathbf{X}^{-1})_{lk}^{(0)} &= \sqrt[4]{\frac{\pi^3}{8}} \frac{1}{\sqrt[4]{A_{x,R}^k A_{y,R}^k A_{z,R}^k}} \delta_{lk}, \\ (\mathbf{X}^{-1})_{lk}^{(1)} &= \sqrt[4]{8\pi^3} \frac{\sqrt[4]{A_{x,R}^k A_{y,R}^k A_{z,R}^k A_{x,R}^l A_{y,R}^l A_{z,R}^l}}{\sqrt[4]{A_{x,R}^k A_{y,R}^k A_{z,R}^k + \sqrt[4]{A_{x,R}^l A_{y,R}^l A_{z,R}^l}}} \\ &\quad \times \frac{c^{kl}}{\sqrt[4]{A_x^{kl}} \sqrt[4]{A_y^{kl}} \sqrt[4]{A_z^{kl}}} (\delta_{k,l-1} + \delta_{k,l+1}). \end{aligned} \quad (\text{B2})$$

The main contribution to the particle number $n_k = (d_{\text{eff}}^k)^* d_{\text{eff}}^k$ is then given by

$$n_k = \sqrt{\frac{\pi^3}{8}} \frac{1}{\sqrt[4]{A_{x,R}^k A_{y,R}^k A_{z,R}^k}} |d^k|^2, \quad (\text{B3})$$

plus terms involving neighboring amplitudes.

The extended variational ansatz is given by

$$\psi = \sum_k d^k e^{-A_x^k x^2 - A_y^k y^2 - A_z^k (z - q_z^k)^2 + i(z - q_z^k) p_z^k}, \quad (\text{B4})$$

with the amplitude $d^k = \exp(-\gamma^k)$. The probability density can then be written as

$$\rho = \sum_{k,l} d^k (d^l)^* e^{-A_x^{kl} x^2 - A_y^{kl} y^2 - A_z^{kl} z^2 + i\tilde{p}_z^{kl} z - \tilde{\gamma}^{kl}}, \quad (\text{B5})$$

with the definitions

$$\tilde{p}_z^{kl} = 2[A_z^k q_z^k + (A_z^l)^* q_z^l] + i(p_z^k - p_z^l), \quad (\text{B6a})$$

$$\tilde{\gamma}^{kl} = A_z^k (q_z^k)^2 + (A_z^l)^* (q_z^l)^2 + i(q_z^k p_z^k - q_z^l p_z^l). \quad (\text{B6b})$$

We integrate ρ over the region discussed in Sec. IV A. The integral over x and y yields

$$\rho_z = \sum_{k,l} d^k (d^l)^* \frac{\pi}{\sqrt[4]{A_x^{kl}} \sqrt[4]{A_y^{kl}}} e^{-A_z^{kl} z^2 + \tilde{p}_z^{kl} z - \tilde{\gamma}^{kl}}. \quad (\text{B7})$$

The integral over z goes over a finite interval, say $a \leq z \leq b$; we can express the result in terms of the error function,

$$\begin{aligned} n(a,b) &= \frac{1}{2} \sum_{k,l} d^k (d^l)^* \frac{\pi^3}{\sqrt[4]{A_x^{kl}} \sqrt[4]{A_y^{kl}} \sqrt[4]{A_z^{kl}}} e^{(\tilde{p}_z^{kl})^2 / 4A_z^{kl} - \tilde{\gamma}^{kl}} \\ &\quad \times \left[\text{erf} \left(\frac{2A_z^{kl} b - \tilde{p}_z^{kl}}{4\sqrt[4]{A_z^{kl}}} \right) - \text{erf} \left(\frac{2A_z^{kl} a - \tilde{p}_z^{kl}}{4\sqrt[4]{A_z^{kl}}} \right) \right]. \end{aligned} \quad (\text{B8})$$

To obtain the number of particles in well i , we evaluate this expression at points a and b between the wells; we can write $a = q_z^i - \ell/2$ and $b = q_z^i + \ell/2$ with ℓ the distance between two wells. As in the case for the four-mode model, the main contribution of the sum results for the summand with $i = k = l$. We get approximately

$$n_i = \sqrt{\frac{\pi^3}{8}} \frac{\text{erf}(\sqrt{A_{z,R}^i} \ell^2 / 2)}{\sqrt[4]{A_{x,R}^i A_{y,R}^i A_{z,R}^i}} |d^i|^2. \quad (\text{B9})$$

For typical values of $A_{z,R}^i \ell^2$ the error function is close to unity. Thus, it is reasonable to compare the particle numbers obtained from the four-mode model [Eq. (B3)] with those from the extended variational ansatz [Eq. (B9)]. Since the particle currents are given by the derivatives of the particle numbers, this is also the case for the particle currents.

- [1] C. E. Rüter, K. G. Makris, R. El-Ganainy, D. N. Christodoulides, M. Segev, and D. Kip, *Nat. Phys.* **6**, 192 (2010).
- [2] Y. D. Chong, L. Ge, and A. D. Stone, *Phys. Rev. Lett.* **106**, 093902 (2011).
- [3] J. Schindler, A. Li, M. C. Zheng, F. M. Ellis, and T. Kottos, *Phys. Rev. A* **84**, 040101 (2011).
- [4] S. Bittner, B. Dietz, U. Günther, H. L. Harney, M. Miski-Oglu, A. Richter, and F. Schäfer, *Phys. Rev. Lett.* **108**, 024101 (2012).
- [5] H. Ramezani, T. Kottos, R. El-Ganainy, and D. N. Christodoulides, *Phys. Rev. A* **82**, 043803 (2010).

- [6] C. M. Bender and S. Boettcher, *Phys. Rev. Lett.* **80**, 5243 (1998).
- [7] S. Klaiman, U. Günther, and N. Moiseyev, *Phys. Rev. Lett.* **101**, 080402 (2008).
- [8] D. Dast, D. Haag, H. Cartarius, G. Wunner, R. Eichler, and J. Main, *Fortschr. Phys.* **61**, 124 (2013).
- [9] Y. Shin, G. B. Jo, M. Saba, T. A. Pasquini, W. Ketterle, and D. E. Pritchard, *Phys. Rev. Lett.* **95**, 170402 (2005).
- [10] H. Cartarius and G. Wunner, *Phys. Rev. A* **86**, 013612 (2012).
- [11] E. M. Graefe, H. J. Korsch, and A. E. Niederle, *Phys. Rev. Lett.* **101**, 150408 (2008).

- [12] D. Haag, D. Dast, A. Löhle, H. Cartarius, J. Main, and G. Wunner, [Phys. Rev. A **89**, 023601 \(2014\)](#).
- [13] A. Zenesini, C. Sias, H. Lignier, Y. Singh, D. Ciampini, O. Morsch, R. Mannella, E. Arimondo, A. Tomadin, and S. Wimberger, [New J. Phys. **10**, 053038 \(2008\)](#).
- [14] C. Elsen, K. Rapedius, D. Witthaut, and H. J. Korsch, [J. Phys. **B 44**, 225301 \(2011\)](#).
- [15] M. Kreibich, J. Main, H. Cartarius, and G. Wunner, [Phys. Rev. **A 87**, 051601\(R\) \(2013\)](#).
- [16] K. Henderson, C. Ryu, C. MacCormick, and M. G. Boshier, [New J. Phys. **11**, 043030 \(2009\)](#).
- [17] A. Trombettoni and A. Smerzi, [Phys. Rev. Lett. **86**, 2353 \(2001\)](#).
- [18] A. Smerzi and A. Trombettoni, [Phys. Rev. **A 68**, 023613 \(2003\)](#).
- [19] I. Bloch, J. Dalibard, and W. Zwerger, [Rev. Mod. Phys. **80**, 885 \(2008\)](#).
- [20] P. Löwdin, [J. Chem. Phys. **18**, 365 \(1950\)](#).
- [21] E.-M. Graefe, [J. Phys. **A 45**, 444015 \(2012\)](#).
- [22] A. D. McLachlan, [Mol. Phys. **8**, 39 \(1964\)](#).
- [23] R. Eichler, D. Zajec, P. Köberle, J. Main, and G. Wunner, [Phys. Rev. **A 86**, 053611 \(2012\)](#).